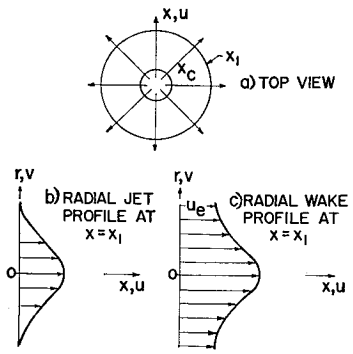

Fig. 1 Schematic diagram

where subscript c denotes conditions at an initial station.

The following boundary-layer compressibility transformation and velocity profile are used:

$$\bar{\rho} dr = \delta_m dn \tag{6a}$$

$$r = \delta_m \int_0^n \frac{dn}{\bar{\rho}} \tag{6b}$$

$$\delta = \delta_m \int_0^1 \frac{dn}{\bar{\rho}} \tag{6c}$$

and

$$u = u_0 + (u_e - u_0) f(n^2) \tag{7}$$

where $\bar{\rho}$ denotes the density divided by its reference value (to be defined), $f(n^2)$ is some function of n^2, and $u_0 = u_0(x)$.

The solutions are presented below.

A. *Radial jets $u_e = 0$*

A1. Laminar flow

$$\frac{3f''(0) \int_{x_c}^{x} \bar{\rho}_0 \bar{\mu}_0 x^2 dx}{(\rho_0 u_0 \delta_m{}^2 x/\mu_0)_c} = \left[1 - \left(\frac{u_{0c}}{u_0}\right)^3\right] \tag{8}$$

where $\bar{\rho} = \rho/\rho_{0c}$, $\bar{\mu} = \mu/\mu_{0c}$, and $f''(0) = (d^2f/dn^2)_0$.

A2. Turbulent flow

$$\frac{2Kf''(0)}{x_c \delta_{mc}} \int_{x_c}^{x} \bar{\rho}_0{}^2 x dx = \left[1 - \left(\frac{u_{0c}}{u_0}\right)^2\right] \tag{9}$$

B. *Radial wakes (u_e = const not equal to zero)*

B1. Laminar flow

$$\frac{f''(0) \int_{x_c}^{x} \tilde{\rho}_0 \tilde{u}_0 x^2 dx}{\rho_e u_e \theta_c{}^2/\mu_e} = F(\tilde{u}_0) - F(\tilde{u}_{0c}) \tag{10a}$$

where $\tilde{\rho} = \rho/\rho_e$, $\tilde{\mu} = \mu/\mu_e$, $\tilde{u} = u/u_e$, and

$$F(\tilde{u}_0) = \frac{2B(2A - B)\tilde{u}_0{}^2 + (2A - B)(A - 3B)\tilde{u}_0 + A(5B - A)}{2(A + B)^3(1 - \tilde{u}_0)^2(A + B\tilde{u}_0)} + \frac{B(B - 2A)}{(A + B)^4} \ln\left(\frac{A + B\tilde{u}_0}{1 - \tilde{u}_0}\right) \tag{10b}$$

The constants A and B only depend on the functional form of $f(n^2)$ and are defined as

$$A = \int_0^1 f(1 - f) dn \qquad B = \int_0^1 (1 - f)^2 dn \tag{10c}$$

B2. Turbulent flow

$$\frac{Kf''(0)}{\theta_c} \int_{x_c}^{x} \tilde{\rho}_0{}^2 x dx = G(\tilde{u}_0) - G(\tilde{u}_{0c}) \tag{11a}$$

Table 1 Asymptotic behavior of flow variables

	Laminar flow		Turbulent flow	
	a	b	a	b
Radial jet	-1	$+1$	-1	$+1$
Radial wake	$-\frac{3}{2}$	$+\frac{1}{2}$	-1	0

where

$$G(\tilde{u}_0) = \frac{-3B^2\tilde{u}_0{}^2 + 2(A^2 + AB + 3B^2)\tilde{u}_0 - (A^2 + 2B^2)}{2(A + B)^3(1 - \tilde{u}_0)^2} + \frac{A^2 + B^2 + AB}{(A + B)^3} \ln\left(\frac{A + B\tilde{u}_0}{1 - \tilde{u}_0}\right) \tag{11b}$$

It is of interest to examine the downstream asymptotic (i.e., as $x \to \infty$) behavior of the velocity along the symmetric axis (u_0) and the semiviscous-layer thickness (δ). If the effect of compressibility can be neglected, the forementioned solutions yield $u_0 \sim x^a$, $\delta \sim x^b$ for the jet and $(u_e - u_0) \sim x^a$, $\delta \sim x^b$ for the wake. Table 1 presents the values of the exponents associated with each of the various types of flows considered herein.

References

[1] Squire, H. B., "Radial jets," *50 Jahre Grenzschichtforschung*, edited by H. Görtler and W. Tollmien (Braunschweig, Vieweg, 1955), pp. 47–54.

[2] Riley, N., "Radial jets with swirl," Quart. J. Mech. Appl. Math. **15**, 435–469 (1962).

Vortices in Solid Propellant Rocket Motors

J. Swithenbank* and G. Sotter†
University of Sheffield, Sheffield, England

Introduction

STUDIES of combustion instability in solid propellant rocket motors currently underway at the High Intensity Combustion Laboratory at Sheffield University have revealed an interesting interaction between the flow pattern and the combustion chemistry. This takes the form of strong vortices in the acoustic cavity which lead to several remarkable effects.

The possible occurrence of these vortices was proposed, largely on theoretical grounds, in an earlier study,[1] and subsequent experimental work has confirmed their existence.

Experimental Evidence

High-speed cinephotos (1000 to 3200 frames/sec) have been taken which show that at least some of the unstable burning pressure peaks are associated with vortices in the flow. Figure 1a shows a typical vortex that filled the entire chamber. From visual observation, the circumferential gas speed is estimated at Mach 0.2 at the fore end, where the picture was taken. The vortex can be expected to gain strength downstream.

Received April 2, 1963. The authors wish to express their thanks to Imperial Metal Industries Ltd., Kidderminster, and to the Ministry of Aviation, who have sponsored this work. The assistance of J. Badger also is acknowledged.

* Lecturer, Department of Fuel Technology and Chemical Engineering.

† Postgraduate Student, Department of Fuel Technology and Chemical Engineering.

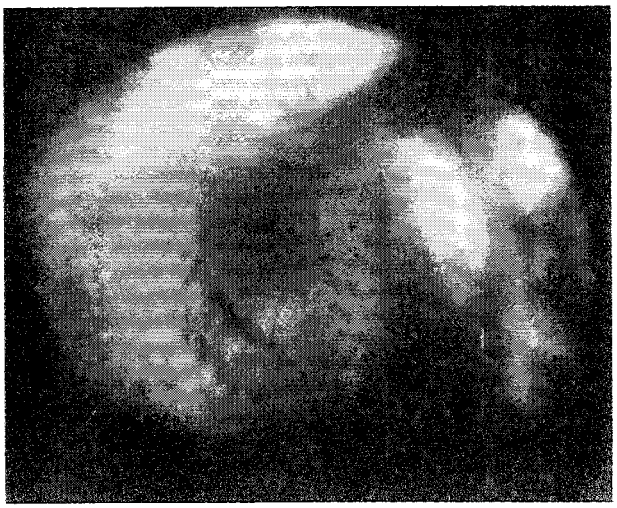

Fig. 1a Print of a frame from a high-speed cinefilm taken during irregular burning in a slotted radial burning charge in cast double-base propellant. Diameter of burning zone is about 3½ in. Rotation is counterclockwise. The motor, with a fore end of perspex, was developed and supplied by the Summerfield Research Station of Imperial Metal Industries Ltd.

Figure 1b shows velocity profiles for acoustic streaming associated with the first transverse traveling mode. Acoustic streaming is a classical phenomenon that has been discussed by Rayleigh[2] and others.[3] In the case of a solid propellant rocket, the flow is altered by transpiration of mass from the propellant surface. The rotating gases are forced toward the center, increasing their speed of rotation to conserve angular momentum. Thus, instead of the linear velocity profile shown in Fig. 1b, a potential vortex is formed, and hence the curving of streamlines in the photograph. The presence of combustion and a rapidly rotating pressure wave suggests that a mechanism such as that of Ref. 1 may be acting to increase vortex strength.

Several such vortices have been observed in various firings and three in the particular firing from which Fig. 1a was made. Their duration is of the order of 0.1 sec, and they correlate with pressure peaks.

Evidence of vorticity in a firing can be obtained also simply by taking standard-speed (24 frames/sec) cinefilms of the motor exhaust; such filming is standard procedure in many test bays. A vortex similar to the one mentioned in the foregoing produced an effect shown in Fig. 1c. This print shows a mild example of the spin that can be imparted to the exhaust gases. In severe cases, axial velocity is so impaired that the "shock triangle" (seen in Fig. 1c) is destroyed or obscured, and the luminous flame begins right at the nozzle opening.

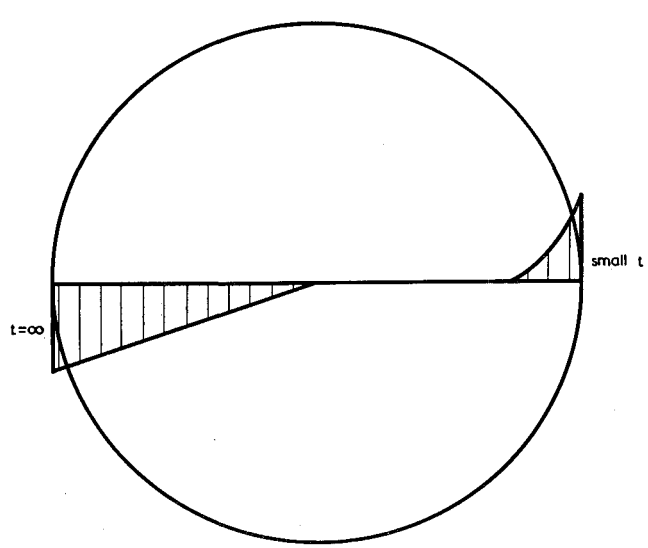

Fig. 1b Velocity profile with respect to radius and to time t for acoustic streaming associated with first traveling tangential mode

Much of the instability of this propellant-motor combination, however, has been associated with the first and second standing tangential modes. Acoustic streaming diagrams for these modes are given in Figs. 2b and 3b. Figures 2a and 3a show smoke patterns produced by solid particles in the combustion products which have been transported to the center following the streamlines shown and have begun to cool and to accumulate carbon particles as they travel back toward the propellant surface. Both the oval and the cruciform shapes are relatively stable, remaining in one orientation for several tenths of a second. They may rotate slowly. In the film in which these shapes were observed, at one period the oval could be seen oscillating between two orthogonal

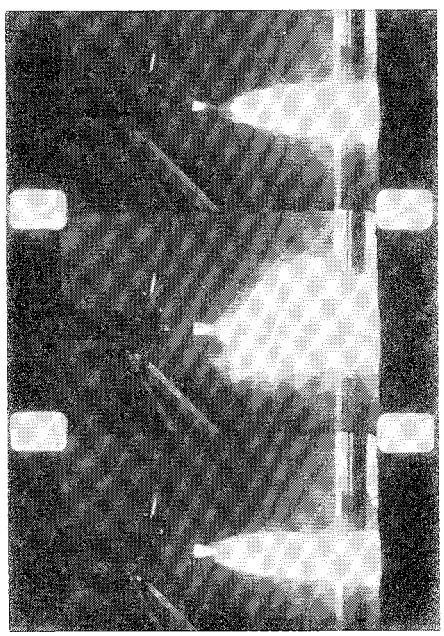

Fig. 1c Cut from 24-frames/sec cinefilm of motor exhaust. These frames were taken during an abnormally high pressure period. Corresponding film of inside of motor showed a vortex at this time of the type shown in Fig. 1a

positions, prior to the second transverse mode's becoming established, for the cruciform appeared shortly thereafter. The change of mode occurs as the higher mode approaches the frequency, corresponding to maximum amplification for this propellant.[4]

The eight vortices formed by the second tangential mode should tend to erode the propellant in eight places around its inner circumference late in the firing; this has, in fact, been observed in this laboratory and in interrupted firings by Trubridge.[5]

Effects Produced by Vortices

The effects produced by vortices are as follows:

1) Erosive burning effects. These usually lead to an increase in chamber pressure.

2) Nozzle effects. In the case of a single vortex (first traveling tangential mode), the effective area of the nozzle throat is reduced seriously,[6] and large increases in chamber pressure may occur. At the higher pressure, the combustion

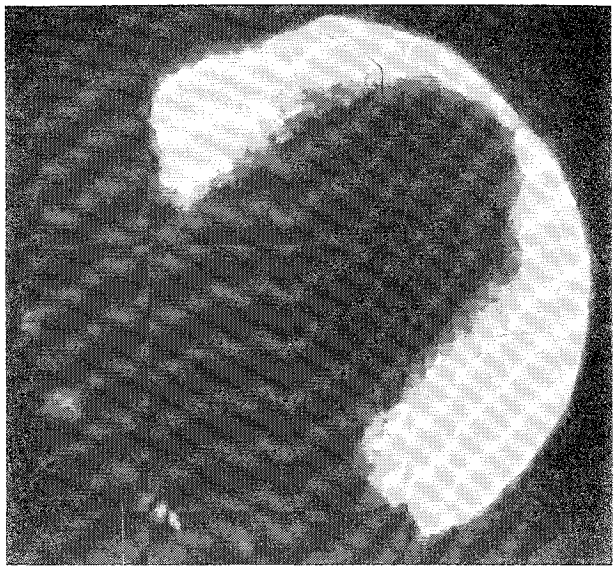

Fig. 2a Oval-shaped smoke pattern (partly obscured by blackening of window) observed in high-speed cinefilm. Axial perforation is circular, about 4 in. in diameter

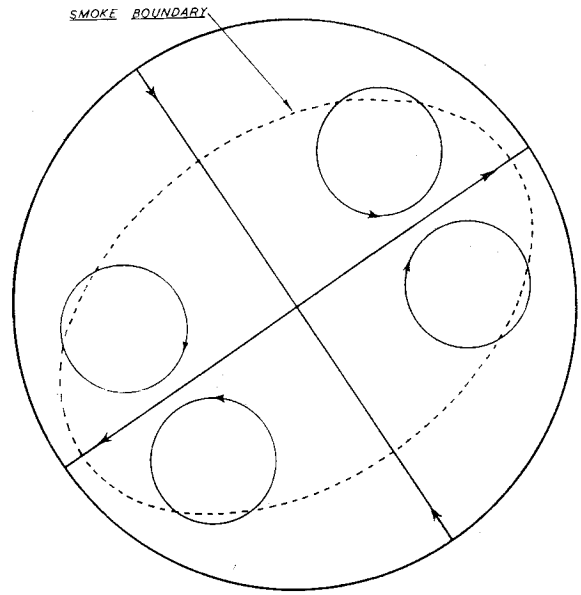

Fig. 2b Acoustic streaming pattern associated with first standing tangential mode, including mass transpiration effects

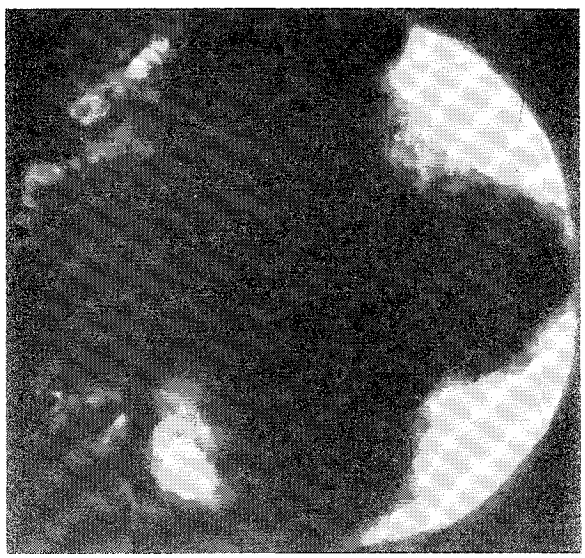

Fig. 3a Cruciform smoke pattern (partly obscured by blackening of window) observed later in firing from which Fig. 2a photograph was taken. Axial perforation is circular, about 4½ in. in diameter

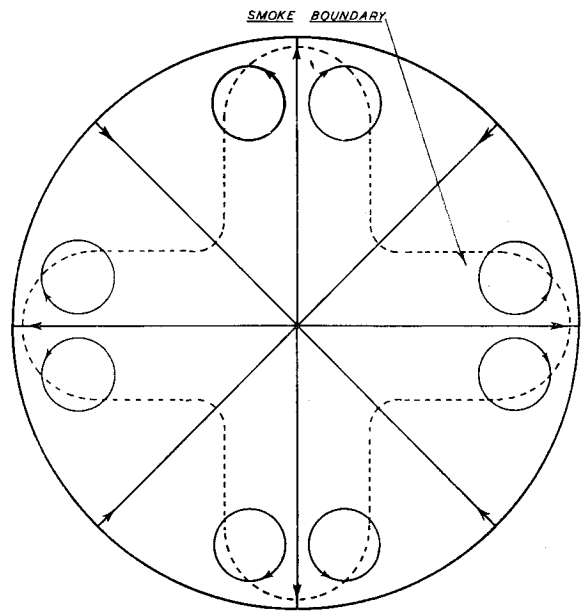

Fig. 3b Acoustic streaming pattern associated with second standing tangential mode, including mass transpiration effects

is usually stable, and this mode appears to be self-annihilating, surviving only about 0.1 sec for the configuration used. Large external noise generation also is evident when the vortex passes through the nozzle.[7]

3) Torque. The single vortex leads to a large torque on the motor case.[8]

Conclusions

More quantitative information is needed to clarify the extent to which vortices contribute to irregular burning. However, there can be little doubt that vorticity is in many instances the long-sought-after "coupling mechanism" between oscillatory and irregular burning.

References

[1] Jenkins, J. M. and Swithenbank, J., "Cyclic combustion driven shocks in a compressible vortex," Rept. 8, High Intensity Combustion Group, Dept. Fuel Technol. and Chem. Eng., Sheffield Univ. (August 1962); also J. Brit. Interplanet. Soc. (to be published).

[2] Rayleigh, J. W. S., *Theory of Sound* (Dover Publications, New York, 1954), Vol. II, p. 333.

[3] Maslen, S. H. and Moore, F. K., "On strong transverse waves without shocks in a circular cylinder," J. Aeronaut. Sci. **23**, 583–593 (1956).

[4] Hart, R. W. and McClure, F. T., "Combustion instability: acoustic interaction with a burning propellant surface," J. Chem. Phys. **30**, 1501–1514 (1959).

[5] Trubridge, G. F. P., "Unstable burning in solid propellant rocket motors," 2nd Rocket Propulsion Symposium, Cranfield, England, Summerfield Res. Station Rept. 62/2, 25 pp. (April 1962).

[6] Mager, A., "Approximate solution of isentropic swirling flow through a nozzle," ARS J. **31**, 1140–1148 (1961).

[7] Jenkins, J. M., "High frequency tangential rocket combustion instability," Ph.D. Thesis, Dept. Fuel Technol. and Chem. Eng., Sheffield Univ. (1963).

[8] Landsbaum, E., "Combustion instability in solid rockets," Jet Propulsion Lab., Calif. Inst. Tech., Rept. 32-146 (1961).